

DTC Sensorless Induction Motor Drives based on MRAS Simultaneous Estimation of Rotor Speed and Stator Resistance

H. Kraiem, M. Ben Hamed, L. Sbita and M. Naceur Abdelkrim
 Research Unit of Modeling, Analysis and Control Systems,
 National School of Engineers of Gabes (ENIG), Tunisia

Abstract: In this study, a sensorless direct torque control scheme for induction motor is proposed. The Luenberger Observer (LO) is designed to estimate the stator currents and rotor flux. The proposed algorithm is applied for high performance induction motor drives without a speed sensor. The estimated stator flux is affected by parameter variations especially the stator resistance due to changes in temperature or frequency. Therefore, it is adequate to compensate this parameter variation using an online adaptation of the control scheme by the estimated stator resistance. For the estimation of the rotor speed and stator resistance, we have designed the Model Reference Adaptive System (MRAS). It has been demonstrated that the Luenberger and MRAS estimation applied to the DTC perform quite well in spite of the parameters and load variations that handled by the system. The simulation results are presented to validate the effectiveness of the overall control scheme.

Key words: Induction motor, direct torque control, Luenberger observer, MRAS, stator resistance estimation

INTRODUCTION

In the recent years, much research interest in Induction Motor (IM) sensorless drives has been developed owing to some of their advantages, such as mechanical robustness, simple construction and maintenance. Present efforts are devoted to improve the sensorless operation, especially for low speed and to develop robust control strategies.

In this area, the Direct Torque Control (DTC) approach initiated by Takahashi (1986) and enhanced by many authors Beum and Blaabjerg (2006) and Vas (1998) offers an interesting issue. It has emerged in 1985 to become one possible alternative to the well-known Vector Control of Induction Machines. Its main characteristic is the good performance, obtaining results as good as the classical vector control but with several advantages based on its simpler structure and control diagram.

The DTC strategy directly controls the inverter states based on the errors between the reference and estimated values of torque and flux. It selects one of 8 voltage vectors generated by a voltage source inverter to keep torque and flux within the limits of 2 hysteresis. Compared with Rotor Field Oriented Control, DTC has many advantages such as less machine parameter dependence, simpler implementation and quicker dynamic torque

response. There is no current controller needed in DTC, because it selects the voltage space vectors according to the errors of flux linkage and torque. The main drawback of the DTC is its relatively high torque and flux ripple.

In the classical DTC, the stator flux vector which is estimated as the integral of the stator voltage vector as described by Eq. (5). It does not depend on motor parameter except the stator resistance. A constant value of stator resistance is considered. However, in practice, this parameter changes due to variation of stator windings temperature. This fact introduces errors in the flux and the electromagnetic torque estimations and the drive may become unstable. So, the compensation for the effect of stator resistance variation then becomes necessary (Vasic *et al.*, 2003; Haque and Rahman, 2000).

Therefore, we propose, in this research, to use the Luenberger Observer and the Model Reference Adaptive System to observe simultaneously the rotor speed and stator resistance. An online adaptation of stator resistance, in the electrical equation to get the stator flux.

BASIC INDUCTION MOTOR MODEL

The dynamic behaviour of an induction motor is described by the following equations written in the α - β referential:

Stator voltage equations:

$$\begin{cases} v_{s\alpha} = R_s i_{s\alpha} + \frac{d\phi_{s\alpha}}{dt} \\ v_{s\beta} = R_s i_{s\beta} + \frac{d\phi_{s\beta}}{dt} \end{cases} \quad (1)$$

Stator flux equations:

$$\begin{cases} \phi_{s\alpha} = L_s i_{s\alpha} + L_m i_{r\alpha} \\ \phi_{s\beta} = L_s i_{s\beta} + L_m i_{r\beta} \end{cases} \quad (2)$$

Electromagnetic torque:

$$J \frac{d\omega_r}{dt} + f_v \omega_r = T_e - T_l \quad (3)$$

Mechanical equation:

$$T_e = n_p \frac{L_m}{\sigma L_s L_r} \phi_s \phi_r \sin \gamma \quad (4)$$

$$\vec{v}_s = [v_{s\alpha} \quad v_{s\beta}]^T, \vec{i}_s = [i_{s\alpha} \quad i_{s\beta}]^T$$

$$\text{and } \vec{\phi}_s = [\phi_{s\alpha} \quad \phi_{s\beta}]^T$$

are represented the stator voltage, current and flux vector. R_s is the stator resistance, L_s , L_r and L_m are the stator, rotor and mutual inductances, n_p the number of pole pairs, T_e and T_l are electromagnetic and load torques, J is the moment of inertia, ω_r is the rotor speed and f_v is the friction factor.

DIRECT TORQUE CONTROL STRATEGY

Direct torque control of induction motor is carried out by hysteresis control of stator flux and torque that directly select one of the 6 non-zero and 2 zero discrete commands of the inverter voltage vectors (Vas, 1998). The selection of the voltage vectors is made so as to restrict the motor stator flux and torque errors within the hysteresis band and obtain the fastest torque response. The selection of the voltage vectors in conventional DTC is based on error outputs produced by the torque and flux hysteresis controllers outputs: τ_f and τ_T what is provided in the form of a switching table as shown in Table 1.

Flux and torque estimation: In the conventional DTC scheme, the stator flux is gotten from (5), which is derived from (1) using only the measured stator voltages and currents (Belhadj, 2004).

Table 1: Optimal switching selection table

		Sectors (S _i : i = 1-6)					
τ_f	τ_T	S ₁	S ₂	S ₃	S ₄	S ₅	S ₆
1	1	V ₂	V ₃	V ₄	V ₅	V ₆	V ₁
	0	V ₇	V ₀	V ₇	V ₀	V ₇	V ₀
	-1	V ₆	V ₁	V ₂	V ₃	V ₄	V ₅
0	1	V ₃	V ₄	V ₅	V ₆	V ₁	V ₂
	0	V ₀	V ₇	V ₀	V ₇	V ₀	V ₇
	-1	V ₅	V ₆	V ₁	V ₂	V ₃	V ₄

$$\vec{\phi}_s = \int (\vec{v}_s - R_s \vec{i}_s) dt \quad (5)$$

This equation is the foundation for implementing the flux estimator. It may be implemented directly, or approximated by various methods to avoid integrator drift. At average and high speed, the voltage drop term ($R_s i_s$) can be neglected, so the stator flux expression becomes:

$$\frac{d\vec{\phi}_s}{dt} = \vec{V}_s \quad (6)$$

Therefore, the stator flux variation is null for a null voltage vector.

$$\frac{d\vec{\phi}_s}{dt} = \vec{0}$$

DTC requires accurate knowledge of the amplitude and angular position for the flux controller:

$$|\vec{\phi}_s| = \sqrt{\phi_{s\alpha}^2 + \phi_{s\beta}^2} \quad \theta_s = \tan^{-1} \left(\frac{\phi_{s\beta}}{\phi_{s\alpha}} \right) \quad (7)$$

The angular position of the stator flux vector must be known so that the DTC can chose between an appropriate set of vector depending on the flux position. The electromagnetic torque can be estimated by using the stator currents measurement and estimated flux as Eq. (8):

$$T_e = n_p (i_{s\beta} \hat{\phi}_{s\alpha} - i_{s\alpha} \hat{\phi}_{s\beta}) \quad (8)$$

Torque and flux hysteresis controllers: The electromagnetic torque value resulting from 8 is then compared with the electromagnetic reference torque, using the 3 level hysteresis controllers. In this manner, the result may be increase, decrease or maintain the torque, depending on the comparator output (Cirincione and Pucci, 2005).

In a similar way, the flux value will be compared with a flux reference, but using a 2 level hysteresis comparator. The result will be used to increase or decrease the flux.

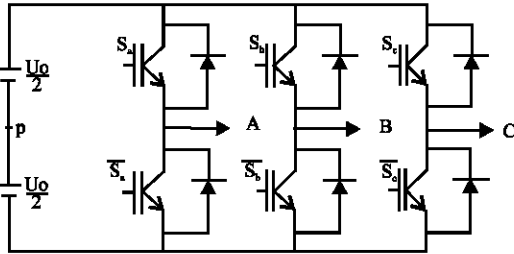


Fig. 1: Three phase PWM inverter switching

Table 2: The modified switching table

		Sectors (S _i : i = 1-6)					
τ_r	τ_T	S ₁	S ₂	S ₃	S ₄	S ₅	S ₆
1	1	V ₂	V ₃	V ₄	V ₅	V ₆	V ₁
	0	V ₆	V ₁	V ₂	V ₃	V ₄	V ₅
0	1	V ₃	V ₄	V ₅	V ₆	V ₁	V ₂
	0	V ₅	V ₆	V ₁	V ₂	V ₃	V ₄

An important factor in these operations is the hysteresis band of the 2 comparators. A too small value may have the effect in loss of the control. The stator flux linkage may exceed the values required by the tolerance band. A narrow window will give better current and flux waveforms but will also increase the inverter switching frequency.

Voltage source inverter : The voltage source inverter can be modeled as shown in Fig. 1, where Sa, Sb, Sc are the switching states (1 in case of switch-on, 0 in case of switch-off). Eight output voltage vectors V_0 to V_7 {000, 100, 110, 010, 011, 001, 101, 111} are obtained for different switch combinations. Hence, V_0 and V_7 are zero voltage vectors (Fig. 2).

The voltage vector of the 3-phase voltage inverters is presented as follows:

$$\bar{V}_s = \sqrt{\frac{2}{3}} U_0 \left(S_a + S_b e^{i\frac{2\pi}{3}} + S_c e^{i\frac{4\pi}{3}} \right) \quad (9)$$

where, A, B and C are the inverter output.

Optimal switching selection table: The combination of the comparator output states, (τ_T , τ_f) and the sector position of the stator flux are used by the optimal switching selection table (Table 1) to chose an appropriate voltage vector to be applied to the inverter.

To simplify the switching table, we supposed that the output of τ_T comparator takes only 2 states, as that of the stator flux (Belhadj, 2004). This means saying that the condition of preservation of the torque is rarely used when the torque reference is inside the hysteresis band. Thus, we can overcome the problem of demagnetization

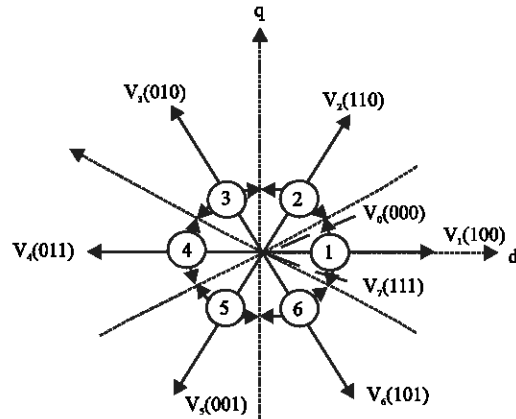


Fig. 2: Different sectors and voltage vectors

caused by the zero voltage vector in the Table 1. The new optimal switching selection table including just active vectors voltage is indicated in Table 2.

THE LUENBERGER OBSERVER

Luenberger Observer is one of the simplest and widely accepted linear observers. It guarantees convergence to real state. LO also enables us to use simplified models and yet get a good performance through an appropriate selection of its gain. The Luenberger Observer shown in this study is a deterministic observer, which is well adapted to a linear, time-variant deterministic system. It uses the errors of the estimated variables compared with the actual variables to correct the errors of the estimated state variables (Ben Hamed and Sbata, 2006). The general equations of Luenberger Observer for the induction motor have the following form:

$$\begin{cases} \hat{\mathbf{x}}(t + T) = \mathbf{A}(t)\hat{\mathbf{x}}(t) + \mathbf{B}(t)\mathbf{u}(t) \\ + \mathbf{L}(t) [\mathbf{y}(t) - \hat{\mathbf{y}}(t)] \hat{\mathbf{y}}(t) = \mathbf{C}\hat{\mathbf{x}}(t) \end{cases} \quad (10)$$

Where the state variables:

$$\begin{aligned} \hat{\mathbf{x}}(t) &= [\hat{x}_1 \quad \hat{x}_2 \quad \hat{x}_3 \quad \hat{x}_4] = [\hat{i}_{sa} \quad \hat{i}_{sb} \quad \hat{\Phi}_{ra} \quad \hat{\Phi}_{rb}] \\ \mathbf{x}(t) &= [x_1 \quad x_2 \quad x_3 \quad x_4] = [i_{sa} \quad i_{sb} \quad \Phi_{ra} \quad \Phi_{rb}] \\ \mathbf{A} &= \begin{bmatrix} a_1 & \omega_s & a_2 & a_3 \omega_r \\ -\omega_s & a_1 & -a_3 \omega_r & a_2 \\ a_4 & 0 & -\frac{a_4}{L_m} & \omega_s - \omega_r \\ 0 & a_4 & -\omega_{sl} & -\frac{a_4}{L_m} \end{bmatrix} \end{aligned}$$

$$\hat{\omega}_r(t) = K_p (e_{i_{\alpha\alpha}}(t)\hat{\phi}_{i\beta}(t) - e_{i\beta}(t)\hat{\phi}_{i\alpha}(t)) + K_i \int (e_{i_{\alpha\alpha}}(t)\hat{\phi}_{i\beta}(t) - e_{i\beta}(t)\hat{\phi}_{i\alpha}(t)) dt \quad (14)$$

where, $e_{i_{\alpha\alpha}}$ and $e_{i_{\beta}}$ are:

$$e_{i_{\alpha\alpha}}(t) = i_{i_{\alpha\alpha}}(t) - \hat{i}_{i_{\alpha\alpha}}(t)$$

$$e_{i_{\beta}}(t) = i_{i_{\beta}}(t) - \hat{i}_{i_{\beta}}(t)$$

Stator resistance estimator: The stator resistance adaptation mechanism (14) is the same as in the customary MRAS speed estimator reviewed in the section before. However, to observe the stator resistance, we have used the cross product of the current error vector and the observed current vector. The adaptive mechanism is given as:

$$\hat{R}_s(t) = K_p (e_{i_{\alpha\alpha}}(t)\hat{i}_{i_{\beta}}(t) - e_{i_{\beta}}(t)\hat{i}_{i_{\alpha\alpha}}(t)) + K_i \int (e_{i_{\alpha\alpha}}(t)\hat{i}_{i_{\beta}}(t) - e_{i_{\beta}}(t)\hat{i}_{i_{\alpha\alpha}}(t)) dt \quad (15)$$

RESULTS

To verify the effectiveness of the proposed sensorless DTC as illustrated in Fig. 3, a digital simulation based on Matlab/Simulink has been carried out. Motor parameters used in simulation are given in Table 3. The used sampling period for simulation is $T = 10^{-4}$ s.

Simulation results are divided into 2 parts: in one hand the operation at low speed region are treated and in the other hand we treat the operation at high speed. These results are given with and without online adjustment of the stator resistance R_s .

The results shown in Fig. 5-6 illustrate, torque, actual and estimated stator flux trajectory, actual and estimated

Table 3: Induction Motor parameters

Power	PN = 3000 W
Nominal voltage	UN = 220/380 V
Frequency	fN = 50 Hz
Stator resistance	$R_s = 2.3 \Omega$
Rotor resistance	$R_r = 1.55 \Omega$
Stator inductance	$L_s = 261 \text{ mH}$
Rotor inductance	$L_r = 261 \text{ mH}$
Mutual inductance	$L_m = 249 \text{ mH}$
Pair pole number	$n_p = 2$
Inertia moment	$J = 0.0076 \text{ kgm}^{-2}$
Friction factor	$f = 0.0007 \text{ N.m.s/rad}$
Sampling period	$T = 0.0001 \text{ ms}$

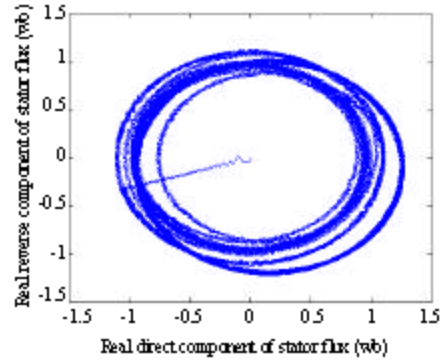


Fig. 5: Operation at low speed without adjustment of R_s 300 rpm. (b) Actual stator flux trajectory

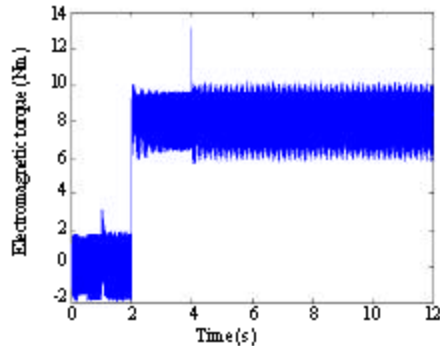


Fig. 5: Operation at low speed without adjustment of R_s 300 rpm. (c) Electromagnetic torque

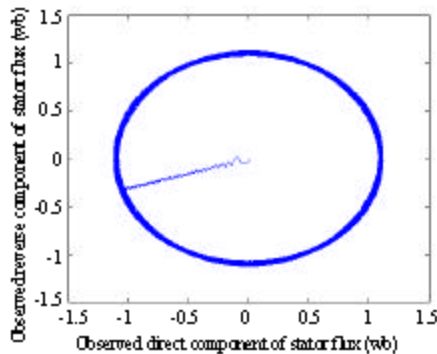


Fig. 5: Operation at low speed without adjustment of R_s 300 rpm. (a) Estimated stator flux trajectory

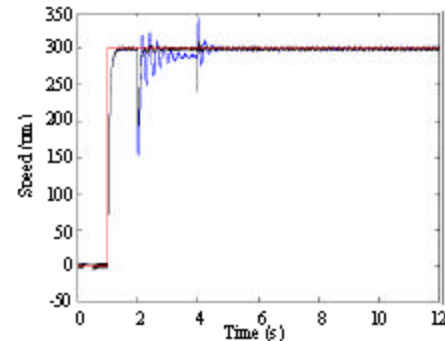


Fig. 5: Operation at low speed without adjustment of R_s 300 rpm. (d) The target, actual and observed

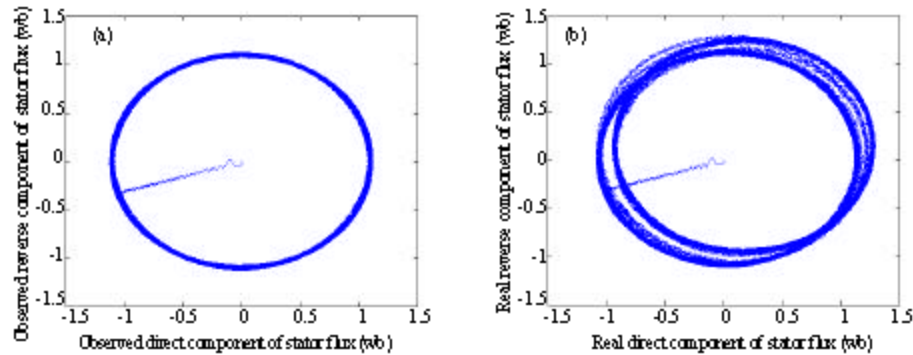


Fig. 6: Operation at low speed with online adjustment of Rs 300 rpm. (a) Estimated stator flux trajectory (b) Actual stator flux trajectory

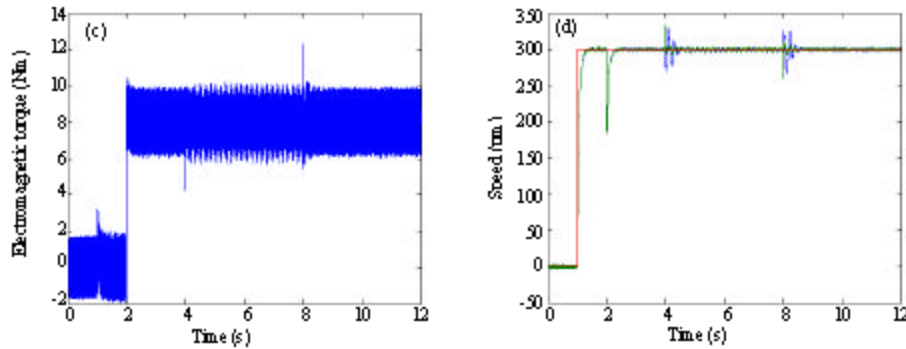


Fig. 6: Operation at low speed with online adjustment of Rs 300 rpm. (b) Actual stator flux trajectory (c) Electromagnetic torque

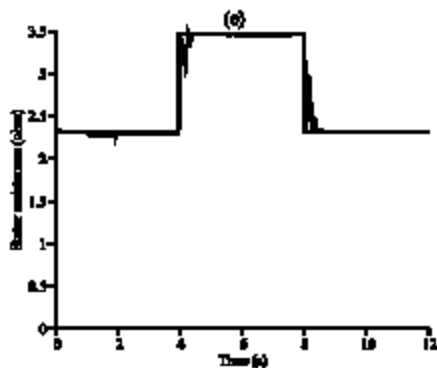


Fig. 6: Operation at low speed with online adjustment of Rs 300 rpm. (e) The actual and estimated stator resistance

rotor speed, actual and estimated stator resistance. In Fig. 5b and d it can be seen the effect of the stator resistance variation, due to the stator resistance increase, the stator flux linkage trajectory is decreased. It can be seen that the sensitivity of the estimated flux trajectory against the stator resistance variation is negligible due to the regulation of the used estimated flux. An error occurs at a time of resistance variation. After the establishment

of this resistance estimation, the error will be canceled due to the online tuning.

Figure 6b show that the stator flux trajectory is kept almost constant in presence of stator resistance variation and this is due to the online adaptation of the control algorithm by the observed stator resistance using the MRAS observer. Torque control dynamic performance of the DTC is shown in Fig. 5c, the ripple affecting both electromagnetic torque response and flux response is due to the use of hysteresis controllers. It can be seen that the stator flux is independent from the torque variations and the estimated flux magnitude follows the commanded value (1.1 Wb). The target speed is changed from 0 rpm to 300 rpm at 1s as shown in Fig. 5d and 6d. The result clearly shows that the estimated speed follows the actual speed and the error is not significant even after the load torque but when the stator resistance is increasing the error becomes remarkable.

Figure 6e shows the simulation result of the estimation stator resistance it is clearly shown that the estimated stator resistance converges to the actual value of R_s with a tiny error (at $t = 4s R'_s = 150\%R_s$ and at $t = 8s R'_s = 100\%R_s$). This result demonstrates that the MRAS observer gives a good estimate for the stator resistance.

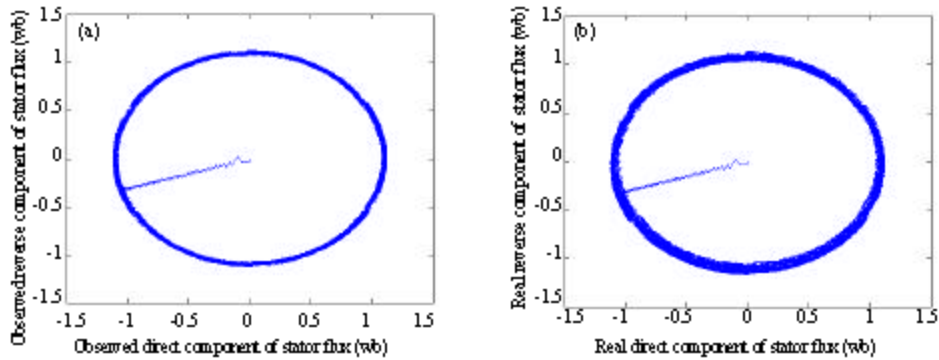


Fig. 7: Operation at high speed without adjustment of R_s (a) Estimated stator flux trajectory (b) Actual stator flux trajectory

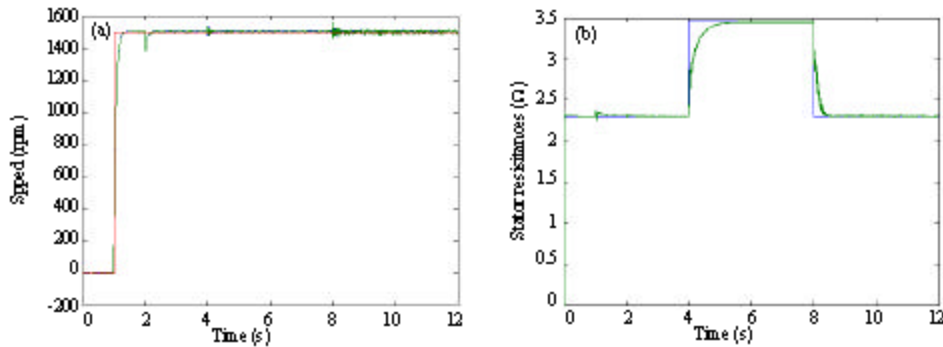


Fig. 8: Operation at high speed with adjustment of R_s . (a) The target, actual and observed speed (b) The actual and estimated stator resistance

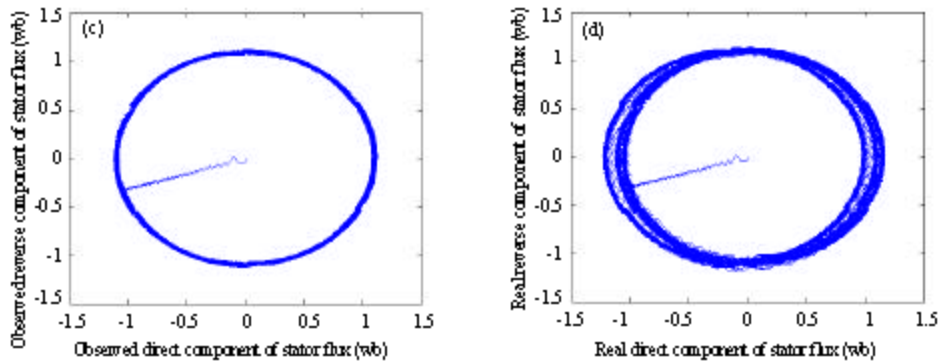


Fig. 8: Operation at high speed with adjustment of R_s . (c) Estimated stator flux trajectory (d) Actual stator flux trajectory

Figure 7 and 8 shows the actual and estimated value of the rotor speed, stator flux and resistance (Operation at high speed $\omega_r = 1500$ rpm). These results almost not affected by the variation of stator resistance then we can say that when we operate at high speed the stator resistance variation can be neglected.

CONCLUSION

In this study, modelling and simulation of Sensorless Direct Torque Control for Induction Motor has been presented. Luenberger Observer and the Model Reference Adaptive System (MRAS) are designed and developed

for use in closed loop control to estimate the rotor speed and flux. To ensure efficiency of the proposed drive especially when we operate at low speed we have online estimate and compensate the stator resistance. The simulation results shows that, the proposed method gives good performance over the wide range of speed. The proposed method, along with its simplicity, has an improved performance in terms of torque and stator flux performances. In a future fellow up research, the proposed scheme is to be implemented on dSpace 1104 controller board.

REFERENCES

- Belhadj, J., 2004. Commande directe en couple d'une machine asynchrone application aux systèmes multimachines multiconvertisseurs. Ph.D. dissertation. Ecole Nationale d'Ingénieurs de Tunis, pp: 185.
- Ben Hamed, M. and L. Sbita, 2006. Speed sensorless indirect stator field oriented control of induction motor based on luenberger observer. Proc. IEEE ISIE06 Conf., pp: 2473-2478.
- Beum, L.K. and F. Blaabjerg, 2006. Reduced-order extended luenberger observer based sensorless vector control driven by matrix converter with nonlinearity compensation. IEEE. Trans. Power Elec., 1 (53): 66-75.
- Cirrincione, M. and M. Pucci, 2005. Sensorless direct torque control of an induction motor by a TLS-based MRAS observer with adaptive integration. Automatica, 11 (41): 1843-1854.
- Haque, M.E. and M.F. Rahman, 2000. The effect of stator resistance variation on direct torque controlled permanent magnet synchronous motor drives and its compensation. The Australasian Universities Power Engineering Conference Brisbane AUPEC'00, pp: 6.
- Kojabali, H.M., L. Chang and R. Doraismi, 2005. A MRAS based adaptative pseudo-reduced order flux observer for sensorless induction motor drives. Elec. Power Components Syst., 4 (20): 930-937.
- Schauder, C., 1992. Adaptive Speed identification for vector control of induction motors without rotational transducers. IEEE. Tran. Ind. Applic., 28: 1054-1062.
- Takahashi, I. and T. Noguchi, 1986. A new quick-response and high-efficiency control strategy for an induction motor. IEEE. Tran. Ind. Applic., 5 (IA-22): 965-970.
- Vas, P., 1998. Sensorless vector and direct torque control. Oxford University Press, pp: 729.
- Vasic, V., S.N. Vukosavic and E. Levi, 2003. A stator resistance estimation scheme for speed sensorless rotor fluxoriented induction motor drives. IEEE. Trans. Energy Conversion, 4(18): 476-483.